Compact Additively Manufactured Conformal Slotted Waveguide Antenna Array

Charalampos Stoumpos, Thierry Le Gouguec, Rozenn Allanic, María García-Vigueras, Anne-Charlotte Amiaud

Compact Additively Manufactured Conformal Slotted Waveguide Antenna Array

Charalampos Stoumpos, Thierry Le Gouguec, Rozenn Allanic, *Member, IEEE*, María García-Vigueras, *Member, IEEE*, and Anne-Charlotte Amiaud

***Abstract*—In this work we present the design and fabrication in metallic 3D-printing of a compact conformal slotted waveguide antenna array operating in the Ku-band. The application objective, although not limited only to this, is the optimisation of an antenna element which by stacking will be able to form a quasi-cylindrical sector. A beamforming network will be used for beam-steering in the elevation plane as coverage in the azimuthal plane is guaranteed by the conformal geometry. The compact design of the antenna element is therefore of great significance. For this reason, a direct feeding scheme by a coaxial connector is adopted. The antenna has been optimized following multiple parametric analyses of its geometrical parameters for the enhancement of the bandwidth, return losses and realized gain. The antenna was fabricated with Selective Laser Melting in aluminium and the experimental results agree well with the numerically calculated ones. The proposed CSWAA exhibits a reflection coefficient below -10 dB, realized gain above 14 dBi, as well as good cross-polarization and side-lobe level over a relative bandwidth of 8%.**

***Index Terms*—Additive Manufacturing, conformal slotted waveguide antenna array, Selective Laser Melting, 3-D printing.**

I. Introduction

CONFORMAL antennas are used in airborne, military and automotive applications as they are placed on fuselages of airplanes/missiles or car bumpers. The compact profile and high RF performance are key aspects. Microstrip antennas have been widely used due to their low profile/cost, light weight as well as feasibility to be placed on conformal surfaces [1]. However, dielectric losses are often a barrier. Slotted waveguide antenna arrays are well-established antenna solutions. Given their high gain/efficiency, low losses and mechanical robustness, they can overcome this limitation [2].

Various design methods and realizations of conformal slotted waveguide antenna arrays (CSWAAs) have been proposed so far in the literature [3]-[9]. These works present the analysis [3]-[6] and design [7]-[9] of slot antennas in the curved broad wall perpendicular to the conformation axis.

Manuscript received January 10, 2023; revised March 09, 2023; accepted April 08, 2023. This work was supported by the Key Technology Domain (KTD) research and innovation program between Thales Group, Lab-STICC and INSA Rennes.

C. Stoumpos and M. García-Vigueras are with the Institute d'Electronique et Télécommunications de Rennes, UMR CNRS 6164, INSA de Rennes, Rennes, France (e-mail: haris_stou@hotmail.com, {charalampos.stoumpos; maria.garcia-vigueras}@insa-rennes.fr).

T. Le Gouguec and R. Allanic are with the Lab-STICC, Université de Bretagne Occidentale, 29238 Brest, France (e-mail: {thierry.legouguec; Rozenn.Allanic}@univ-brest.fr).

A. -C. Amiaud is with Thales LAS France SAS, 78990 Élancourt, France (e-mail: anne-charlotte.amiaud@thalesgroup.com).

Digital Object Identifier 10.1109/LAWP.2023.xxx

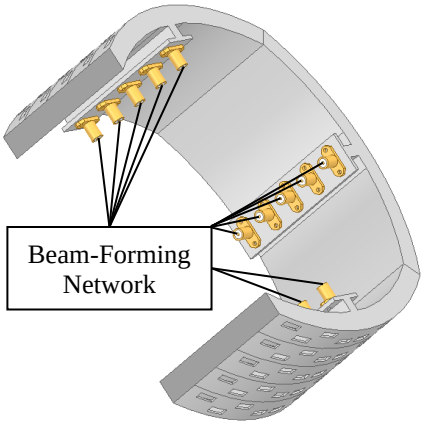

Fig. 1. Application example of a cylindrical 4×5 array composed by the proposed CSWAA and a Beam-Forming Network (BFN) for scanning in elevation.

Metal additive manufacturing (AM) or 3D-printing is a significant breakthrough in the field of antennas and microwave networks in waveguide technology [10]. It allows to benefit from very low losses and high power-handling, while at the same time, the design freedom to shape waveguides like in the case of CSWAAs is much higher and the cost typically lower with respect to the conventional manufacturing techniques [11].

Various slotted waveguide antenna array realizations in AM have been reported in the literature. These refer to automotive radar applications [12], planar topologies of slot-excited [13]-[14] or cavity-backed slotted waveguide antennas [15]-[16], leaky-wave [17]-[18] and frequency scanning [19] solutions. A work that evaluates and highlights the feasibility and adaptability of metallic 3D-printing for Ku-band planar cavity corporate-fed waveguide antenna array is also found in [20].

3D-printed CSWAA designs refer to proactive CSWAAs for beam shaping [21], dual-polarized and dual-band conical-beam cross-slotted cylindrical waveguide antenna arrays [22] and omnidirectional solutions for 5G applications in Selective Laser Melting (SLM) [23]. A first investigation on waveguide-fed linear and planar CSWAAs with the slots being parallel to the conformation axis has been communicated in [24]-[25]. On one hand, these works focus on the fabrication parameters, such as the machine settings, the parts orientation, the material roughness as well as the geometrical accuracy and how these degrade the EM performance. On the other hand, these CSWAAs are narrowband as the design process was out of these works scope. Last, the followed fabrication approach post-analyzed and presented in these papers led to severe geometrical deformations and significant RF degradation.

This article has been accepted for publication in IEEE Antennas and Wireless Propagation Letters. This is the author's version which has not been fully edited and content may change prior to final publication. Citation information: DOI 10.1109/LAWP.2023.3266376

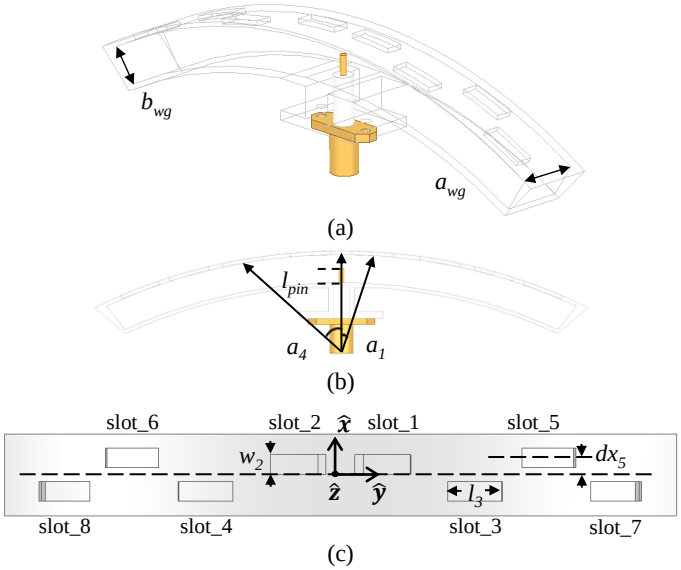

Fig. 2. Geometry and design variables of the CSWAA: (a) perspective wireframe view, (b) side wire frame view and (c) opaque top-view.

The application domain is related to the concept published in [26] by some of this paper's authors. This work focuses on airborne and missile applications and how CSWAAs used in 3-D Active Electrically Scanned Arrays (AESAs) are capable of replacing the mechanical beam-steering systems with faster, less expensive and more compact ones. A representative application example is depicted in Fig. 1, where the proposed CSWAA is used to form a cylindrical 4×5 array connected to a beamforming network (BFN) for scanning in elevation (coverage in the azimuthal plane is assured by the system's conformal geometry). We present here the design and AM of a compact and highly efficient CSWAA (8% operating bandwidth), able to be used in such applications of 3-D AESAs.

The rest of the paper is structured as follows. Section II deals with the geometry, design and optimization of the CSWAA. In section III, the fabrication and measurements are presented and discussed. The paper closes with the conclusions of this work.

II. Design and Analysis of the CSWAA

The design frequency band of the CSWAA is Ku-band (f_0 = 14.5 GHz) with a minimum specified fractional bandwidth of 5%. The minimum targeted realized gain is 14 dBi (minimum aperture efficiency of 50%). Last, the conformation angle and radius have been fixed to 60° and 120 mm, respectively.

A. Antenna Structure and Initial Analysis

The antenna's layout is depicted in Fig. 2(a). The main metallic body is in wireframe view, the coaxial conducting parts are in yellow and the dielectric part in white. The direct coaxial feeding mechanism has been used here [27]. This provides wideband operation, while at the same time presents a highly compact footprint which is of great significance for the targeted application (Fig. 1). Fig. 2(b) shows the wireframe side cut-view of the proposed CSWAA and Fig. 2(c) the top view.

The initial design of the antenna is first explained here. From Fig. 2, the fixed geometrical parameters are: a_{wg}=12.5 mm (0.34λ_g), b_{wg}=8 mm (0.22λ_g) (λ_g = 36.78 mm). The rest relate to the slots width (w), length (l), radial position from each slot's center (a) and mutual displacement with reference to (w.r.t.) x-axis (dx). The simulations were performed by ANSYS HFSS.

At the first optimization round, the variables w and l were kept fixed and equal to 1 mm and 9.9 mm, respectively. Besides, the variable dx was the same for all slots in order to reduce the number of iterations. At this stage, the slots' radial position (a_i) was analyzed for different values of dx. The 1st design included: dx_{all}=3.3 mm and $a_{1,2}$ = 3.55°, $a_{3,4}$ = 10.65°, $a_{5,6}$ = 17.9°, $a_{7,8}$ = 25.4°. This gives an equal distance between the slots w.r.t. y-axis. Fig. 3, shows that although this design case proves to be rather broadband in terms of S_{11}, the realized gain remains below 13.5 dBi. After simulations for lower x-axis and radial distance between the slots, the 2nd design included: dx_{all}=2 mm and $a_{1,2}$ = 3.65°, $a_{3,4}$ = 10.95°, $a_{5,6}$ = 18.3°, $a_{7,8}$ = 25.1°. In this case, the S_{11} remains broadband while the realized gain remains above 13.5 dBi. The 3rd design included the optimized for this stage variable dx_{all}=2.4 mm and slightly larger radial values $a_{1,2}$ = 3.75°, $a_{3,4}$ = 11.25°, $a_{5,6}$ = 18.75°, $a_{7,8}$ = 25.1°. From Fig. 3(b), the 3rd design's realized gain remains above 14 dBi over a bandwidth of 4% at the expense of a slightly less broadband S_{11}.

B. Final Parametric Analysis and Optimization

The proposed CSWAA was finally subjected to multiple parametric analyses so as to maximize the return losses and the realized gain for a minimum bandwidth of 5%. The results of this exhaustive study are shown in Fig. 4.

The most critical design parameters refer to a and dx. These allow the appropriate spatial modulation of the slots which compensates for the degradation to the radiation performance produced by the conformation when typical design approaches are adopted. In particular, Fig. 4(a) shows that the slots length have low impact on the antenna's performance. Although not shown for brevity, this is also the case for the variable w. Figs. 4(b)-(c) show that the slots radial position is determinant on the band of interest and the bandwidth itself, except for the two slots 7 and 8. Likewise, as observed from Figs. 4(d)-(f), the mutual displacement (dx) is equally critical for the proper selection of the band as well as the realized gain enhancement within this band. The optimized geometrical parameters are:

- $a_{1,2}$ = 3.65°, $a_{3,4}$ = 11.7°, $a_{5,6}$ = 18.25°, $a_{7,8}$ = 24.5°
- l_i = 9.92 mm ≈ 0.27λ_g, i=1,…,8
- w_i = 3.5 mm ≈ 0.095λ_g, i=1,…,8
- $dx_{1,2}$ = 1.8 mm ≈ 0.049λ_g, dx_j = 3 mm ≈ 0.082λ_g, j=3,…,8
- l_{pin} = 4.13 mm ≈ 0.11λ_g

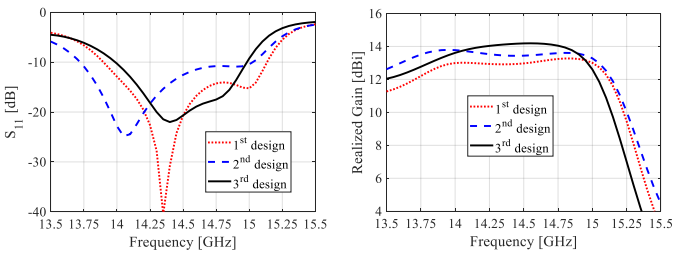

Fig. 3. Initial parametric analysis of the CSWAA's with three design cases: (a) reflection coefficient and (b) realized gain.

This article has been accepted for publication in IEEE Antennas and Wireless Propagation Letters. This is the author's version which has not been fully edited and content may change prior to final publication. Citation information: DOI 10.1109/LAWP.2023.3266376

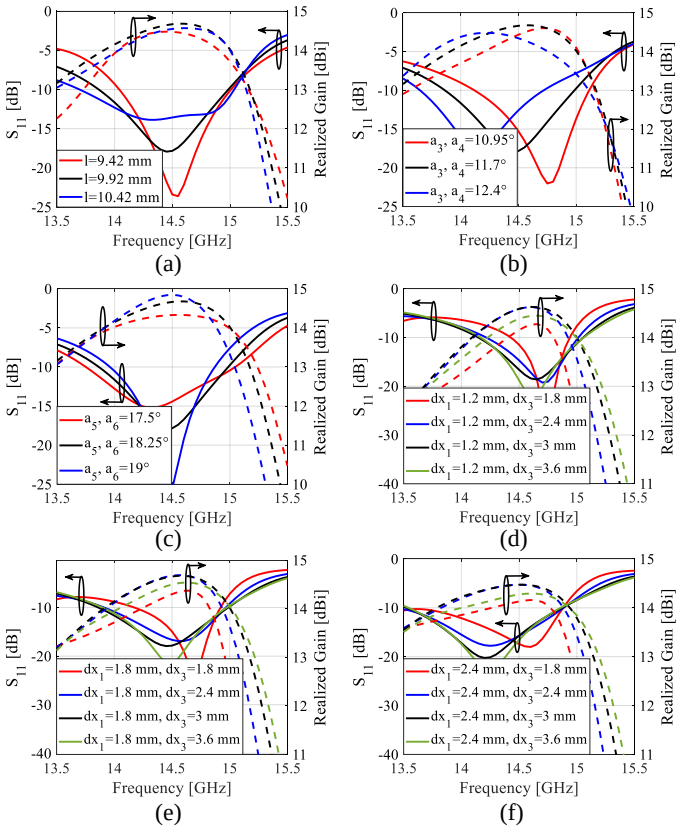

Fig. 4. Parametric analysis of the CSWAA's critical design variables: (a) slots length (*l*), (b)-(c) slots 3-6 position w.r.t. *y*-axis from Fig. 2(c) and (d)-(f) slots position w.r.t. *x*-axis from Fig. 2(c).

III. Fabrication and Experimental Results

Two prototypes of the proposed CSWAA were fabricated by our industrial partner *Thales 3D Morocco* in order to address the repeatability of the process. The printer that was used is the quad-laser Formup350 from ADDUP. The thickness of the waveguide walls is 1 mm and the body of the antenna was produced monolithically by four laser fibers that solidify layer-by-layer the aluminum powder (AlSi10Mg). The manufacturing tolerances are of the order of ±150μm. The two 3D-printed in SLM prototypes of the proposed CSWAA are shown as built at the left part of Fig. 5(a). These raw prototypes were then machined so as to remove the lattice structure below used to support the antenna during the printing process. The final antenna structure with its coaxial connector is shown in the bottom right part of Fig. 5(a).

The most important parameter for the antenna's fabrication is its orientation during the printing process. After trials and past experience [10]-[11], [24]-[25] with the SLM process, we concluded to the optimal orientation; that which produces the least manufacturing risk related to overhanging metallic regions. So, w.r.t. Fig. 5(b), the optimal positioning of the CSWAA is as follows. The CAD model was first rotated 45° around the x-axis and then a 45° rotation around the y-axis was performed. This technique, proves to be very crucial with respect to the structural stability of the antenna during the fabrication process as it orients every part of it to a maximum inclination angle of 45° as a worst case. This essentially means that overhangs that would occur for larger than 45° angles are avoided.

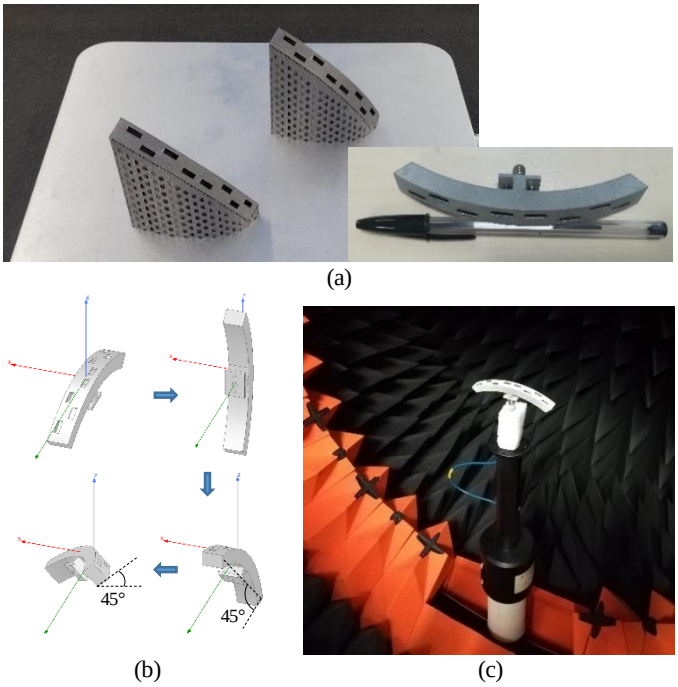

Fig. 5. Prototyping and measurements: (a) Two 3D-printed in SLM prototypes of the proposed CSWAA as built (left) and the antenna with its connector (right). (b) Orientation approach for fabrication. (c) The measurement setup in the anechoic environment of MVG StarLab.

The experimental characterization of the CSWAA has been performed in the anechoic environment of the near-field compact-range multi-probe Over-The-Air testing system MVG / Satimo StarLab [Fig. 5(c)]. The prescribed efficiency and realized gain uncertainty levels vary from ±0.7 to ±0.9 dB between 10-20 GHz.

The experimental results of the two CSWAA prototypes are presented in Figs. 6 and 7. The simulated and measured S_{11} of is shown in Fig. 6(a). The results show a close agreement. The S_{11} is lower than -10 dB over 14-15 GHz. The slightly lower reflection level of the measured prototypes is attributed to mechanical tolerances of the SLM process as well as to the losses of the prototypes. Figs. 6(b) and 6(c) show the simulated and measured broadside realized gain as well as the total and aperture efficiency over the frequency, respectively. A close agreement between numerical and experimental results is observed. The antenna's realized gain, total and aperture efficiency remain above 14 dBi, 90% and 50% over the bandwidth of interest (14-15 GHz), as prescribed by the minimum requirements in Section II. The slight deviations of the measurements are attributed to manufacturing tolerances, while the ripples as well as the gain and efficiency values exceeding simulated ones and 100%, respectively, are due to non-idealities in the positioning of the antenna under test (AUT) in the center of the chamber's arc as well as uncertainties of the measurement system owing to non-ideal calibration and systematic errors. Such discrepancies are commensurate with what is reported in the literature [10], [15], [18]-[20]. The AUT was positioned in the center of the arc of StarLab using a foam structure [Fig. 5(c)] and was later fixed with adhesive tape. However, slight vibrations during the azimuthal rotation of the testbench could not be totally eliminated. The deviations between measured and simulated values are around ±0.5 dB,

which is less than the uncertainty level prescribed by StarLab.

The surface roughness of the fabrication depends on the process parameters as well as the orientation of the printed part [25], [28]-[29]. In Ku-band and for printing in 45°, the surface roughness is of the order of 5–20 μm Ra [30], inducing an equivalent electrical resistivity of ρ = 20 $\mu\Omega$·cm [31]. These values are in line with former works of microwave components in SLM [32], as well as in our case. In particular, Fig 6(b) shows the simulated and measured (prot. 2) ohmic (finite conductivity and connector) and mismatch losses at 14-15 GHz. Simulations show average ohmic losses of 0.12 dB and mismatch losses of 0.1~0.4 dB, while measurements average ohmic losses of 0.2 dB and mismatch losses of 0.1~0.3 dB. Both the simulated and measured average total losses are around 0.35 dB at 14-15 GHz.

The last experimental results of the proposed 3D-printed CSWAA relate to its E-plane (φ=0°) and H-plane (φ=90°) radiation patterns and are illustrated in Fig. 7. In particular, the co-polarized realized gain radiation patterns over the lowest, central and highest frequencies are depicted in Figs. 7(a)-(c), while the cross- polarized ones in Figs. 7(d)-(f), respectively. Both numerically calculated and experimental results show a good agreement. An increase in the measured cross-polarized level is also observed and is attributed to potential asymmetries produced by the fabrication process and non-ideal positioning w.r.t. the azimuthal orientation during the measurements.

According to simulations, the cross-polarized radiation level at φ=2°~5° is around -10 dB, which is consistent with the measured values. Prototype 2 presents a slightly better cross-polarized level. Tomographic analyses of both prototypes may shed light on these aspects.

IV. Conclusion

In this letter, we present the design, optimization, additive manufacturing in SLM and experimental characterization of a highly compact Ku-band CSWAA. This type of antenna is suitable for AESA antennas which is an excellent candidate for airborne and missile applications. The parametric analyses and fabrication pre-analysis are also presented in this work. The experimental results of the proposed CSWAA agree well with the simulations. The antenna presents reflection loss above 10 dB and realized gain above 14 dBi over a fractional bandwidth of 8% with the central frequency of operation being 14.5 GHz.

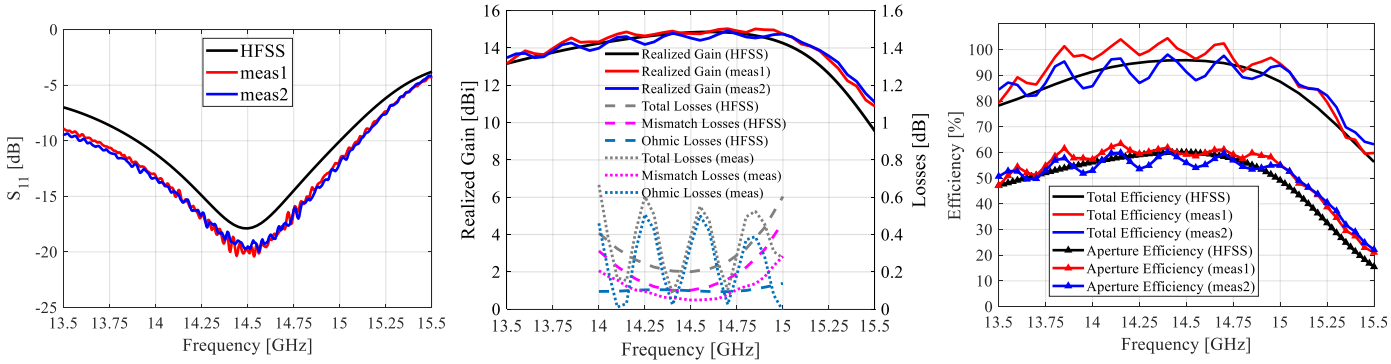

Fig. 6. Simulation and experimental results of the CSWAA: (a) Reflection coefficient, (b) realized broadside gain & losses, (c) total & aperture efficiency.

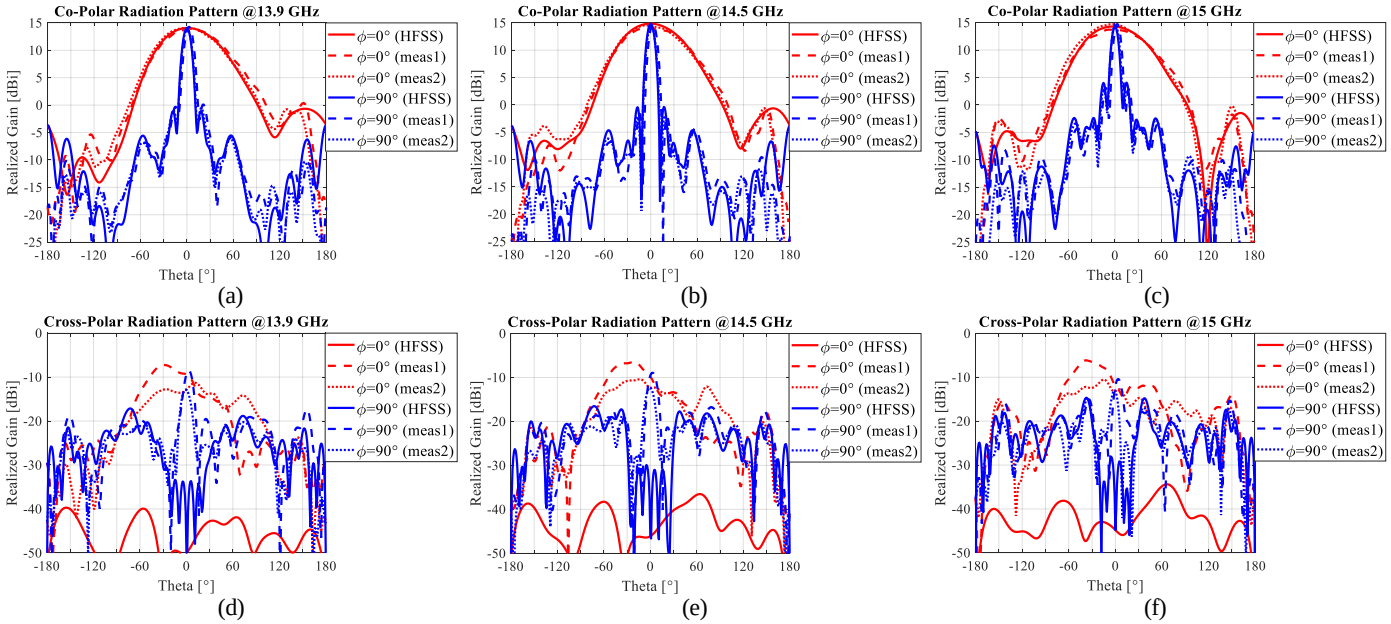

Fig. 7. Simulated and measured radiation patterns (cuts at φ=0° and φ=90°) of the CSWAA: (a) Co-polar pattern at 13.9 GHz, (b) Co-polar pattern at 14.5 GHz, (c) Co-polar pattern at 15 GHz, (d) Cross-polar pattern at 13.9 GHz, (e) Cross-polar pattern at 14.5 GHz and (f) Cross-polar pattern at 15 GHz.

REFERENCES

[1] L. Josefsson and P. Persson, *Conformal Array Antenna Theory and Design.* John Wiley & Sons, Inc., Hoboken, New Jersey, 2006.

[2] R. Elliott and L. Kurtz, "The design of small slot arrays," *IEEE Trans. Antennas Propag.*, vol. 26, no. 2, pp. 214-219, Mar. 1978.

[3] C. W. Westerman, V. L. Harrington and P. K. Park, "Analytic design of conformal slot array", *IEEE Trans. Antennas Propag.*, vol. 31, no. 4, pp. 668-672, Jul. 1983.

[4] S.-W. Lue, S.-C. Li and S.-M. Cao, "Slot antenna in the curved broad wall of a sectoral waveguide," *Proc. Asia-Pacific Microwave Conf. (APMC 92)*, vol. 1, pp. 401–403, Aug. 1992.

[5] M. Kalfa and V. B. Ertürk, "Analysis of slotted sectoral waveguide arrays with multilayered radomes", *IEEE Trans. Antennas Propag.*, vol. 64, no. 2, pp. 800-805, Feb. 2016.

[6] H. Yang *et al*., "Design equations for cylindrically conformal arrays of longitudinal slots", *IEEE Trans. Antennas Propag.*, vol. 64, no. 1, pp. 80-88, Jan. 2016.

[7] M. -p. Jin, M. -q. Qi, W. Wang and X. -l. Liang, "Design of a cylindrically conformal waveguide-fed slot array antenna," *Proc. IEEE Int. Symp. Antennas Propag.*, pp. 1053-1054, Jul. 2014.

[8] Y. Liu, H. Yang, Z. Jin, F. Zhao and J. Zhu, "A multibeam cylindrically conformal slot array antenna based on a modified rotman lens," *IEEE Trans. Antennas Propag.*, vol. 66, no. 7, pp. 3441-3452, Jul. 2018.

[9] A. Traille, J. Ratner, G. D. Hopkins and V. Tripp, "Development of a novel faceted conformal slotted-waveguide subarray for sensor applications with full 360° azimuth tracking capabilities", *Proc. IEEE Antennas Propag. Soc. Int. Symp.*, pp. 3828-3831, Jun. 2007.

[10] Stoumpos, C., J. -P. Fraysse, G. Goussetis, R. Sauleau and H. Legay, "Quad-Furcated Profiled Horn: The Next Generation Highly Efficient GEO Antenna in Additive Manufacturing," *IEEE Open J. Antennas Propag.*, vol. 3, pp. 69-82, 2022.

[11] M. García-Vigueras, L. Polo-Lopez, C. Stoumpos, A. Dorlé, C. Molero and R. Gillard, "Metal 3D-Printing of Waveguide Components and Antennas: Guidelines and New Perspectives", in Hybrid Planar - 3D Waveguiding Technologies [Working Title]. London, United Kingdom: IntechOpen, 2022.

[12] K. Lomakin, M. Sippel, K. Helmreich and G. Gold, "3D printed slotted waveguide array antenna for D-band applications", *Proc. 15th Eur. Conf. Antennas Propag. (EuCAP)*, pp. 1-4, Mar. 2021.

[13] G. P. Le Sage, "3D printed waveguide slot array antennas," *IEEE Access*, vol. 4, pp. 1258-1265, 2016.

[14] Y. Wu, B. Jiang, M. Zhang, J. Hirokawa and Q. H. Liu, "A four-corner-fed slotted waveguide sparse array for near-field focusing", *IEEE Access*, vol. 8, pp. 203048-203057, 2020.

[15] G.-L. Huang, S.-G. Zhou, T.-H. Chio and T.-S. Yeo, "Fabrication of a high-efficiency waveguide antenna array via direct metal laser sintering", *IEEE Antennas Wireless Propag. Lett.*, vol. 15, pp. 622-625, 2016.

[16] Z. Chen, S.-G. Zhou and T.-H. Chio, "A class of all metal cavity-backed slot array with direct metal laser sintering", *IEEE Access*, vol. 6, pp. 69650-69659, 2018.

[17] A. Dorle *et al.*, "Additive manufacturing of modulated triple-ridge leaky-wave antenna", *IEEE Antennas Wireless Propag. Lett.*, vol. 17, no. 11, pp. 2123-2127, Nov. 2018.

[18] A. Dorle *et al.*, "Circularly polarized leaky-wave antenna based on a dual-mode hollow waveguide", *IEEE Trans. Antennas Propag.*, vol. 69, no. 9, pp. 6010-6015, Sep. 2021.

[19] K. Zhao, J. A. Ramsey and N. Ghalichechian, "Fully 3-D-Printed frequency-scanning slotted waveguide array with wideband power-divider", *IEEE Antennas Wireless Propag. Lett.*, vol. 18, pp. 2756-2760, 2019.

[20] E. García-Marín, J. L. Masa-Campos, P. Sánchez-Olivares and J. A. Ruiz-Cruz, "Evaluation of additive manufacturing techniques applied to Ku-band multilayer corporate waveguide antennas", *IEEE Antennas Wireless Propag. Lett.*, vol. 17, no. 11, pp. 2114-2118, Nov. 2018.

[21] Y. F. Wu, H. R. Zhang, Y. J. Cheng and Y. Fan, "Proactive conformal waveguide slot array antenna to synthesize cosecant squared pattern based on 3-D printing manufacturing process," *IEEE Trans. Antennas Propag.*, vol. 70, no. 8, pp. 6627-6634, Aug. 2022.

[22] P. Sanchez-Olivares, J. L. Masa-Campos and E. Garcia-Marin, "Dual-polarization and dual-band conical-beam array antenna based on dual-mode cross-slotted cylindrical waveguide", *IEEE Access*, vol. 9, pp. 94109-94121, 2021.

[23] P. Sanchez-Olivares, E. Garcia-Marin and J. L. Masa-Campos, "Direct metal laser sintering conformal waveguide array antenna for millimeter-wave 5G communications," *IEEE Antennas Wirel. Propag. Lett.*, vol. 21, no. 5, pp. 1012-1016, May 2022.

[24] A. Guennou-Martin *et al.*, "Design and manufacturing of a 3-D conformal slotted waveguide antenna array in Ku-band based on direct metal laser sintering", *Proc. IEEE Conf. Antenna Meas. Appl. (CAMA)*, pp. 1-4, Oct. 2016.

[25] A. Martin-Guennou *et al.*, "Direct metal laser sintering process investigation: application to 3D slotted waveguide antennas", *IET Microw. Antennas Propag.*, vol. 11, no. 14, pp. 1921-1929, Nov. 2017.

[26] S. Abedrrabba *et al.*, "DRAGON: Adaptive RF seekers based on 3-D conformal antennas," *Proc. Int. Radar Conf. (RADAR)*, pp. 1-6, Sep. 2019.

[27] H. C. Zhao, R. R. Xu and W. Wu, "Broadband waveguide slot array for SAR", *Electron. Lett.*, vol. 47, no. 2, pp. 76-77, Jan. 2011.

[28] Calignano, F. *et al.*: "Influence of process parameters on surface roughness of aluminum parts produced by DMLS", *Int. J. Adv. Manuf. Technol.*, 2013, 67, pp. 2743–2751.

[29] K. Kamarudin, M. S. Wahab, Z. Shayfull, A. Ahmed and A. A. Raus, "Dimensional Accuracy and Surface Roughness Analysis for AlSi10Mg Produced by Selective Laser Melting (SLM)", *MATEC Web Conf.*, vol. 78, pp. 1-8, Oct. 2016.

[30] A. Maamoun, Y. Xue, M. Elbestawi and S. Veldhuis, "Effect of Selective Laser Melting Process Parameters on the Quality of Al Alloy Parts: Powder Characterization, Density, Surface Roughness, and Dimensional Accuracy," *Materials*, vol. 11, no. 12, p. 2343, Nov. 2018.

[31] O. Paverini *et al.*, "Additive manufacturing of Ku/K-band waveguide filters: a comparative analysis among selective-laser melting and stereolithography," *IET Microw. Antennas Propag.*, vol. 11, no. 14, pp. 1936-1942, Nov. 2017.

[32] O. Paverini *et al.*, "Selective Laser Melting Manufacturing of Microwave Waveguide Devices," *Proc. IEEE*, vol. 105, no. 4, pp. 620-631, Apr. 2017.